Mfsd14a (*Hiat1*) gene disruption causes globozoospermia and infertility in male mice.

Joanne Doran[1], Cara Walters[2], Victoria Kyle[2], Peter Wooding[2], Rebecca Hammett-Burke[2], William Henry Colledge[+2].

[1]Takeda Cambridge Ltd

418 Science Park

Milton Road

Cambridge

CB4 0PZ

UK

[2]Department of Physiology, Development and Neuroscience

University of Cambridge

Downing Street

Cambridge

CB2 3EG

UK

[+]Corresponding Author

Tel: 01223 333881

Fax: 01223 333840

E-mail: whc23@cam.ac.uk

Short Title: *Mfsd14a* disruption causes globozoospermia.

Abstract

The *Mfsd14a* gene, previous called *Hiat1*, encodes a transmembrane protein of unknown function with homology to the solute carrier protein family. To study the function of the MFSD14A protein, mutant mice (*Mus musculus*, strain 129S6Sv/Ev) were generated with the *Mfsd14a* gene disrupted with a *LacZ* reporter gene. Homozygous mutant mice are viable and healthy but males are sterile due to a 100-fold reduction in the number of spermatozoa in the vas deferens. Male mice have adequate levels of testosterone and show normal copulatory behaviour. The few spermatozoa that are formed show rounded head defects similar to those found in humans with globozoospermia. Spermatogenesis proceeds normally up to the round spermatid stage but the subsequent structural changes associated with spermiogenesis are severely disrupted with failure of acrosome formation, sperm head condensation and mitochondrial localization to the mid-piece of the sperm. Staining for β-galactosidase activity as a surrogate for *Mfsd14a* expression indicates expression in Sertoli cells suggesting that they may transport a solute from the bloodstream that is required for spermiogenesis.

Introduction

Spermatogenesis is the developmental process by which spermatozoa are produced from spermatogonial germ cells in the gonads (Grootegoed, et al. 1995, Jan, et al. 2012). At the start of this process, spermatogonial cells give rise to primary spermatocytes, which progress through meiosis to produce haploid spermatids. The spermatids subsequently undergo spermiogenesis, a complex series of morphological changes to form spermatozoa (Toshimori and Ito 2003). During spermiogenesis, chromatin condensation and nuclear remodelling occur and formation of the acrosome that contains glycosylated enzymes essential for egg fertilization. The acrosome is formed by fusion of pro-acrosomal vesicles, derived from the Golgi apparatus, which fuse to form a cap structure over the nucleus. A flagellum with the central 9 + 2 microtubular axoneme is also formed during spermiogenesis and contains a mid-piece packed with mitochondria to provide energy for motility.

Defects in spermiogenesis contribute to male infertility problems in humans. Globozoospermia is one such syndrome that is found in around 0.1% of infertile men (Dam, et al. 2007a). The disorder is characterized by round-headed sperm with a disrupted acrosome and abnormal mitochondrial localization. Genes that cause globozoospermia have been identified in mutant mice and include *Atg7*(Wang, et al. 2014), *Ck2*(Xu, et al. 1999), *Dpy19l2*(Pierre, et al. 2012), *Gopc*(Yao, et al. 2002), *Hrp*(Kang-Decker, et al. 2001), *Hsp19β1*(Audouard and Christians 2011), *Pick1*(Xiao, et al. 2009), *Smap2*(Funaki, et al. 2013), and *Spaca1*(Fujihara, et al. 2012) and *Vps54* (Paiardi, et al. 2011). Of these, causative mutations have been identified in humans including *DPY19L2* (Harbuz, et al. 2011, Koscinski, et al. 2011), *PICK1* (Liu, et al. 2010) and *SPATA16* (Dam, et al. 2007b).

The *Mfsd14a* (a.k.a. *Hiat1*) gene was originally identified as an abundant transcript isolated from a fetal mouse hippocampus cDNA library (Matsuo, et al. 1997) and classified as a member of the major facilitator superfamily of solute carrier proteins (SLCs) (Sreedharan, et al. 2011). The SLC's

consist of a large group of proteins capable of transporting diverse substances including amino acids, sugars, nucleosides, and fatty acids (Hediger, et al. 2004). The *Mfsd14a* gene shows modest sequence homology with the *E.coli* tetracycline resistant protein class C (31%) and with the mouse GLUT2 and GLUT4 glucose transporters (29%). Furthermore, the protein has a similar structure to existing sugar transporters; 12-transmembrane spanning α-helices, the sugar transporter specific D-R/K-X-G-R-R/K motif between the 2nd and 3rd transmembrane domains and a region similar to the facilitative glucose transporter specific P-E-S-P-R motif at the end of the 6th transmembrane domain. These characteristics suggest that the *Mfsd14a* gene may encode a novel sugar transporter but the solute specificity of the protein is not known.

To establish the physiological function of the MFSD14A protein *in vivo*, we generated a transgenic mouse line with a *LacZ* gene insertion that disrupts expression of the *Mfsd14a* gene. Phenotypic characterization of these mutant mice indicated that the MFSD14A protein is required for the spermiogenesis stage in sperm formation whereby round spermatids are structurally remodelled into spermatozoa.

Materials and Methods.

Gene targetting and generation of mutant mice.

The transgenic mice were generated by standard methods in collaboration with Takeda Cambridge. The targetting vector was constructed using homology arms amplified from 129S6/Sv/Ev mouse genomic DNA using the following primers:

5'armF: CCAACAAATAAGAGAGCGCTGCCTGTG;

5'armR: ACCAATAAGTGGGGCACTGAGGAATG;

3'armF: CTCTGATGAAGATCAGCCCGTGGTAAG;

3'armR: GCAGTAAGCCAGCCTGGGTATAGTAAAG.

The 5'armF/R primers amplified a 1.54-kb fragment, and the 3'armF/R primer pair amplified a 3.9-kb fragment. The arms were cloned on either side of a cassette containing an IRESLacZ reporter gene and a promoted neomycin phosphoribosyltransferase selectable marker gene. Homologous recombination of this targetting construct results in the deletion of 70bp of exon 4 of the *Mfsd14a* locus, which changes the coding frame to one that contains 23 stop codons and terminates translation of the MFSD14A protein at Glycine 93.

ES cells (CCB; 129S6/SvEv strain) were cultured, and gene targetting was performed as described previously(Ratcliff, et al. 1992). Targetted clones were identified by PCR. Chimeras were generated by injection into C57/Bl6 blastocysts, and inbred mice were established by breeding germ-line chimeras with 129S6/Sv/Ev mice.

Animals.

All experiments were performed in accordance with the relevant guidelines and regulation under the authority of a United Kingdom Home Office Project Licence and were approved by the Local Ethical Review Committee of the University of Cambridge.

Genotyping transgenic mice.

Mice were genotyped by PCR using genomic DNA from ear biopsies. Genotyping primers were:

Mutant *Mfsd14a* allele, Forward Primer: GTCTGGGACCAGCCCTTTAT

Mutant *Mfsd14a* allele, Reverse Primer: TGGCGAAAGGGGGATGTG

Wild-type *Mfsd14a* allele, Forward Primer: GTCTGGGACCAGCCCTTTAT

Wild-type *Mfsd14a* allele, Reverse Primer: ACGAGCAGGTAAAGGCTCAA

RT-PCR.

Total RNA was prepared from testes using a SV Total RNA Isolation kit Z3101 (Promega, Southampton, UK) and converted into cDNA using a GoScript™ Reverse Transcription Kit, A5000 (Promega) according to the manufacturer's instructions. All primer pairs spanned introns to eliminate any amplification from genomic DNA and RNA samples were included without a reverse transcription step as a negative control. Primer pairs were: mHprtF (CAGGCCAGACTTTGTTGGAT)/ mHprtR (TTGCGCTCATCTTAGGCTTT), 147 bp product;
mMfsd14aEx1F (ATGACCCAGGGGAAGAAAAAG)/ mMfsd14aEx3R (GGTTTCATGCAATACCACCA), 195 bp product;
mMfsd14aEx4F (GTTTGGGGCCGAAAGTCC)
mMfsd14aEx5R (GCAAAAACCCCAGAAACAGA), 119 bp product.
The amplification cycle was: 95 ^{0}C, 5 min, (93 ^{0}C, 0.5 min, 60 ^{0}C, 0.5 min, 70 ^{0}C, 1min) x40.

Sperm and germ cell counts

Mice were killed and sperm isolated from a fixed length of the vas deferens by squeezing into 100 µl of 1% PBS. A 25 µl sample was loaded onto a haemocytometer and the number of sperm counted. For quantitation of germ cells, haematoxylin and eosin stained sections at stages IV/V/VI of the seminiferous cycle were photographed at the same magnification and the number of each germ cell type counted in a 100 µm x 200 µm rectangle drawn on the photomicrograph. Counts

were made from 49 rectangles for wild-type mice (n=4) and from 48 rectangles for mutant mice (n=4).

Testosterone ELISA

Total plasma testosterone levels were measured in wild-type and mutant mice at approximately 3 months of age using a commercially available ELISA kit (DRG International, USA, EIA-1559) according to the manufacturer's instructions. The analytical sensitivity of the ELISA was 0.083 ng/ml, the intra-assay variation 3.2% and the inter-assay variation 6.7%. 100µl of blood was collected from the vena cava and mixed with 2 µl of 0.5M ethylene-di-amine-tetra-acetic acid (EDTA) anti-coagulant. Plasma was obtained by centrifugation of the sample at 16,500 g for 5 minutes and stored at -80 ^{o}C until assayed. Plasma samples were assayed without further extractions so that the free testosterone levels were measured.

Histology.

Tissues were fixed in 4% paraformaldehyde/PBS overnight at 4^{o}C, dehydrated through graded alcohols, and embedded in wax or epoxy resin for histological sectioning. Wax sections were cut at 7 µm and stained with haematoxylin and eosin. For visualization of acrosome formation, resin sections (1 µm) were stained with 1% toluidine blue in 70% ethanol. Mitochondria were visualized with MitoTracker® Green (Invitrogen). To detect β-galactosidase activity, tissues were fixed in 4% paraformaldehyde/PBS for 30 minutes, washed in PBS and incubated overnight at 37^{o}C in LacZ stain (5mM potassium ferricyanide, 5 mM potassium ferrocyanide in PBS, 20 mg/ml X-gal stock and 1 mM $MgCl_2$). The samples were post-fixed in 4% paraformaldehyde/PBS prior to wax embedding and sectioning. For electron microscopy, tissues were fixed in 4% glutaraldehyde, postfixed in 1% osmium tetroxide, *en bloc*-stained with 2% uranyl acetate, dehydrated, and

embedded in Spurr's epoxy.

Statistical analyses.

The statistical tests are indicated in the Figure legends. For data sets that did not pass a normality test, a non-parametric test was used (two-tailed, Mann-Whitney). A P-value of less than 0.05 was taken to be significant.

Results.

The *Mfsd14a* gene was disrupted by gene targetting in mouse ES cells to remove 70 bp of coding sequence from exon 4 and insert an IRES (Internal Ribosome Entry Site)-LacZ-Neo reporter gene (Fig. 1A). Transgenic mutant mice carrying this targetted *Mfsd14a* allele (designated *Mfsd14a*^{tm1Coll}) were generated and tested by RT-PCR to confirm a null allele (Fig. 1B). RT-PCR between exons upstream of the insertion (P1F/P3R) generated the expected 195bp product in both wild-type and mutant mice (Fig. 1B). RT-PCR across the insertion site, between exons 3 and 5, generated a 197bp product in wild-type mice and a 69bp product in the mutant mice (Fig. 1B). Sequence analysis of the PCR product from the mutant mice indicated that this was from mRNA that had spliced between exon 3 and 5. RT-PCR using a forward primer located within the 70bp deleted sequence and a downstream primer (P4F/P5R) gave an 119bp product in wild-type but no product in the mutant mice indicating that no wild-type transcripts were present in the mutant mice (Fig. 1B). All PCR products were sequenced to confirm their identity.

The disrupted *Mfsd14a* allele contains an IRES-*LacZ* reporter gene, which is expressed from the endogenous *Mfsd14a* promoter (Fig. 1A). This allows the expression profile of the *Mfsd14a* gene to be examined at the cellular level by staining tissues for β-galactosidase activity. This is useful as no suitable antibodies are available to visualise expression of the MFSD14A protein by immunohistochemistry. Expression of the *Mfsd14a* gene was confirmed in the hippocampus (Fig.

1D) as previously reported (Matsuo, et al. 1997). *Mfsd14a* gene expression was also found in the testes with the distribution of β-galactosidase activity often spread throughout the seminiferous tubule and highest close to Sertoli cell nuclei (Fig. 1D, arrowed). These observations are consistent with *Mfsd14a* expression in Sertoli cells with no indication of expression in germ cells.

The *Mfsd14a* mutant mice were overtly healthy with no obvious signs of any detrimental phenotype. Mutant females were fertile but mutant males were sterile. The average body weight of the mutant male mice was slightly slower than that of age-matched wild-type mice (26.6 ± 2.0g versus 28.9 ± 1.8g, Table 1). Consequently, tissue weights were normalized relative to body weight (Table 1). There were no significant differences between wild-type and mutant mice in the relative weights of the liver, kidney, testis, epididymis or vas deferens but the weight of the seminal vesicle was slightly less in the mutant mice (Table 1). Free testosterone levels were not significantly different between mutant and wild-type mice although two wild-type mice had higher levels than the rest of the cohort (Fig. 2A). The mutant mice showed normal copulatory behaviour and produced vaginal plugs after mating (Fig. 2B). The number of sperm that could be isolated from the vas deferens was around 100-fold lower in the mutant mice ($5.0 \times 10^6 \pm 1.0 \times 10^6$) compared to wild-type ($4.3 \times 10^8 \pm 5 \times 10^7$) (Fig. 2C). Quantitation of each type of germ cell in the testes at stage V of the seminiferous cycle indicated that there was no difference in the number of spermatogonia, primary spermatocytes or round spermatids but the number of elongating spermatids was significantly lower in the mutant mice (Fig. 2D).

Histological analysis of the testes of mutant mice showed that the process of spermiogenesis was severely disrupted. The mutant mice showed dysmorphic sperm head formation with abnormal nuclear condensation (Fig. 3B) compared to the condensed heads of wild-type mice (Fig. 3A, arrowed). The mutant sperm showed formation of a tail however (Fig. 3J). The number of sperm in the epididymis of the mutant mice was less than in wild-type mice (Fig. 3C and D) and the round-

216 headed shape of the sperm with residual cytoplasm was clearly visible. Toluidine blue staining for
217 glycoproteins showed that the mutant sperm did not form an acrosome compared to the normal
218 acrosomal cap over the nucleus of the wild-type sperm (Fig. 3G-H). At stage I of the seminiferous
219 cycle, prior to any acrosome development, step 1 spermatids appeared identical in wild-type and
220 mutant testes (Fig. 3E and F). In contrast, at stage VI of the seminiferous cycle, the acrosome is
221 clearly visible in the wild-type mice (Fig. 3G) but no acrosome has formed in the mutant mice (Fig.
222 3H). Small vesicles that stain for glycoproteins are found in the mutant mice suggesting a defect in
223 vesicular trafficking from the Golgi and/or fusion with the developing acrosome. Sperm isolated
224 from the vas deferens of mutant mice showed a round head, irregular shaped nucleus and absence of
225 a distinct mid-piece compared to wild-type sperm (Fig. 3I and J). Wild-type sperm showed normal
226 localization of mitochondria to the mid-piece (Fig. 3 K and M). In contrast, mutant sperm failed to
227 localize mitochondria to the mid-piece and mitochondria were often found in the head region (Fig.
228 3 L and N).
229
230 Ultrastructural analysis by transmission electron microscopy confirmed the light microscopy
231 findings that the morphological changes associated with spermiogenesis were disrupted in the
232 mutant mice. At Step 1 of spermiogenesis, no obvious difference was observed between normal and
233 mutant spermatids (Fig. 4A). By Step 6 of spermiogenesis, wild-type sperm showed the early stage
234 of acrosome formation with a single pro-acrosomal granule within the growing acrosome (Fig. 4B).
235 In contrast, the mutant mice show no acrosome formation and the presence of several small pro-
236 acrosomal granules (Fig. 4B). Both wild-type and mutant mice show a thickening of the nuclear
237 membrane opposite the Golgi complex that gives rise to the acrosomal vesicles suggesting correct
238 formation of the acroplaxome. Mitochondria were found in the head of both wild-type and mutant
239 sperm at this stage. By Step 9 of spermiogenesis, the sperm heads showed considerable
240 morphological remodelling, with condensation and elongation of the nucleus, and removal of
241 excess cytoplasm (Fig. 4C). At this stage, the manchette, a microtubule structure involved in

242 nuclear reshaping (Yoshida, et al. 1994) was clearly visible. At Step 9, mutant sperm had no
243 acrosome formation and the nuclear remodelling was disrupted with abnormal vacuolation of the
244 nucleus but they showed formation of the manchette (Fig. 4C). By Step 13, wild-type sperm
245 showed the typical elongated sperm head shape with a clear acrosome (Fig. 4D). In contrast, the
246 mutant sperm at this stage had irregular shaped nuclei with mitochondria in close proximity and no
247 obvious acrosome formation (Fig. 4D). Mutant sperm isolated from the epididymis showed round
248 heads with residual cytoplasm (Fig. 4D) while the wild-type sperm had condensed heads with clear
249 acrosomal caps and no residual cytoplasm.
250

Discussion

We have shown that the *Mfsd14a* gene is required for the final stages of spermatogenesis in mice, namely the structural remodelling of round spermatids into functional spermatozoa. Mutant mice have severely reduced sperm numbers in the vas deferens and are sterile. While this reduction in sperm numbers alone would render the mice sub-fertile, the lack of an acrosome will also prevent egg fertilization as the acrosome contains enzymes required for penetration through the zona pellucida of the egg. The number of sperm observed in the cauda epididymis is also reduced suggesting that release of sperm into the seminiferous tubules (spermiation) is impaired. Spermiation can be impaired by a low testosterone level (Beardsley and O'Donnell 2003) but this is unlikely to be the case for the *Mfsd14a* mutant mice as they have testosterone levels sufficient to allow development of accessory sex organs and normal copulatory behaviour.

In the absence of a suitable antibody for immunohistochemistry, the expression profile of the targetted *Mfsd14a* gene was visualized by staining for β-galactosidase activity. The staining was consistent with expression in Sertoli cells rather than the germ cell themselves. β-galactosidase activity was found to extend throughout the inside of the seminiferous tubules, presumably within the Seroli cell cytoplasm, but was also concentrated close to Sertoli cell nuclei in the peri-tubular compartment. Sertoli cells play a major role in supporting germ cell development and Sertoli-germ cell junctions allow communication between these cell types. Disruption of acrosome formation by a Sertoli cell-specific gene defect is not unprecedented. For example, disruption of the *Gba2* gene, which encodes a β-glucosidase enzyme located in the endoplasmic reticulum of Sertoli cells, results in round-headed sperm lacking acrosomes (Yildiz, et al. 2006). β-glucosidase hydrolyzes glucosylceramide, a glycolipid, into glucose and ceremide. In the *Gba2* mutant mice, glucosylceramide accumulates in the Sertoli cells but it is not known if this is derived from the germ cells or produced by the Sertoli cells themselves. Whatever the mechanism, the *Gba2* mutant mice illustrate that a Sertoli cell defect can result in globozoospermia.

Other mutant mice have been described with defects in acrosome biogenesis and globozoospermia including those with disruption of the *Atg7*(Wang, et al. 2014), *Ck2*(Xu, et al. 1999), *Dpy19l2*(Pierre, et al. 2012), *Gopc*(Yao, et al. 2002), *Hrb*(Kang-Decker, et al. 2001), *Hsp19β1*(Audouard and Christians 2011), *Pick1*(Xiao, et al. 2009), *Smap2*(Funaki, et al. 2013), *Spaca1*(Fujihara, et al. 2012) and *Vps54* (Paiardi, et al. 2011) genes. The similarity in the phenotype of these mutant mice suggests that these genes form a functional network required for the ultrastructural changes to the sperm head. One common cell process in which several of these proteins are involved is in vesicle trafficking in the cell. During acrosome formation, vesicles bud from the trans-Golgi network and bind to the acroplaxome, a mesh of cytoskeletal fibres covering the surface of the sperm nucleus (Kierszenbaum and Tres 2004). These pro-acrosomal vesicles eventually fuse to form the acrosome. PICK and GOPC co-localize to trans-Golgi vesicles (Xiao, et al. 2009) and PICK1 as been shown to bind to both GOPC and CK2α. The *Atg7* gene encodes a protein that is required to localize GOPC to the trans-Golgi vesicles (Wang, et al. 2014). Similarly, *Smap2* encodes a GTPase activating protein that interacts with clathrin (Natsume, et al. 2006) and is required for vesicle budding from the trans-Golgi network(Funaki, et al. 2013). *Hrb* also encodes a GTPase activating protein which is localized to the cytoplasmic side of proacrosomal vesicles and is involved in their fusion (Kang-Decker, et al. 2001). The *Vps54* gene encodes a vesicle sorting protein involved in retrograde transport of endosomes to the trans-Golgi network.

Appropriate sorting, trafficking and fusion of intracellular vesicles to the correct subcellular location is a complex process involving many different proteins. How the MFSD14A protein fits into this pathway to regulate acrosome formation and sperm maturation is not yet known. Since the MFSD14A protein has homology to sugar transporters, it is possible that defects in protein or lipid glycosylation may play a role in this process. Glycosylation is an important post-translational modification important in protein sorting to different cell compartments. For example, mannose-6-

phosphate residues on glycoproteins are important in targetting these proteins to lysosomes. It has been suggested that acrosome biogenesis is functionally related to the formation of secretory lysosomes (Hartree 1975, Moreno and Alvarado 2006). The acrosome contains several enzymes that are also found in lysosomes (eg. acid phosphatase, Cathepsin D and H) and the contents of both organelles are acidified by a vacuolar H^+-pump (V-ATPase).

Interestingly, DPY19L2 is a putative C-Mannosyltransferase based on homology to the *C. elegans* gene dumpy-19 (*Dpy19*). *Dpy19L2* mutant mice do not form an acrosome and show defective chromatin compaction during spermiogenesis with defective transport of protamines into the nucleus (Yassine, et al. 2015). Based on these data, one hypothesis is that MFSD14A is required for uptake of a sugar (eg mannose) from the bloodstream by the Sertoli cells, which is then used by spermatids for glycosylation of key molecules required for acrosome formation. It may be informative to perform a glycomics analysis of the *Mfsd14a* mutant testes to gain an insight into the substance that is transported by this protein.

Our data show that the *Mfsd14a* gene is required for the structural remodelling events required to produce spermatozoa in mice. The MFSD14A protein sequence is very similar between mice and other species including mammals (99.8%), reptiles (95%), amphibians (93%), birds (84%) and fish (82%). This suggests that the function of this protein is conserved across several classes of vertebrates. The mutant mice produce reduced sperm numbers with round heads very similar to those observed in infertile men with rare cases of globozoospermia(Dam, et al. 2007a). The similarity between the sperm from the mutant mice and those produced in human globozoospermia extends to a failure to produce the acrosome and to correctly localize mitochondria to the mid-piece of the sperm. These close similarities suggest that some globozoospermia men will have mutations in the *MFSD14A* gene and we are currently screening individuals for this mutation.

Declaration of Interest

The author(s) declare no competing financial interests.

Funding.

This research did not receive any specific grant from any funding agency in the public, commercial or not-for-profit sector. This work was funded by a Ford Physiology Fund Endowment (WHC).

Acknowledgements.

We would like to thank the biofacility staff, particularly Wendy, for exemplarity husbandry.

Author Contributions

JD and WHC generated the KO mouse line, CW, VK, and RH-B characterized the phenotype, PW performed the electron microscopy, WHC designed the study and wrote the manuscript. All authors reviewed the manuscript.

References

Audouard, C, and E Christians 2011 Hsp90beta1 knockout targetted to male germline: a mouse model for globozoospermia. *Fertil Steril* **95** 1475-1477 e1471-1474.

Beardsley, A, and L O'Donnell 2003 Characterization of normal spermiation and spermiation failure induced by hormone suppression in adult rats. *Biol Reprod* **68** 1299-1307.

Dam, AH, I Feenstra, JR Westphal, L Ramos, RJ van Golde, and JA Kremer 2007a Globozoospermia revisited. *Hum Reprod Update* **13** 63-75.

Dam, AH, I Koscinski, JA Kremer, C Moutou, AS Jaeger, AR Oudakker, H Tournaye, N Charlet, C Lagier-Tourenne, H van Bokhoven, and S Viville 2007b Homozygous mutation in SPATA16 is associated with male infertility in human globozoospermia. *Am J Hum Genet* **81** 813-820.

Fujihara, Y, Y Satouh, N Inoue, A Isotani, M Ikawa, and M Okabe 2012 SPACA1-deficient male mice are infertile with abnormally shaped sperm heads reminiscent of globozoospermia. *Development* **139** 3583-3589.

Funaki, T, S Kon, K Tanabe, W Natsume, S Sato, T Shimizu, N Yoshida, WF Wong, A Ogura, T Ogawa, K Inoue, N Ogonuki, H Miki, K Mochida, K Endoh, K Yomogida, M Fukumoto, R Horai, Y Iwakura, C Ito, K Toshimori, T Watanabe, and M Satake 2013 The Arf GAP SMAP2 is necessary for organized vesicle budding from the trans-Golgi network and subsequent acrosome formation in spermiogenesis. *Mol Biol Cell* **24** 2633-2644.

Grootegoed, JA, WM Baarends, PJ Hendriksen, JW Hoogerbrugge, KE Slegtenhorst-Eegdeman, and AP Themmen 1995 Molecular and cellular events in spermatogenesis. *Hum Reprod* **10 Suppl 1** 10-14.

Harbuz, R, R Zouari, V Pierre, M Ben Khelifa, M Kharouf, C Coutton, G Merdassi, F Abada, J Escoffier, Y Nikas, F Vialard, I Koscinski, C Triki, N Sermondade, T Schweitzer, A Zhioua, F Zhioua, H Latrous, L Halouani, M Ouafi, M Makni, PS Jouk, B Sele, S Hennebicq, V Satre, S Viville, C Arnoult, J Lunardi, and PF Ray 2011 A recurrent deletion of DPY19L2 causes infertility in man by blocking sperm head elongation and acrosome formation. *Am J Hum Genet* **88** 351-361.

Hartree, EF 1975 The acrosome-lysosome relationship. *J Reprod Fertil* **44** 125-126.

Hediger, MA, MF Romero, JB Peng, A Rolfs, H Takanaga, and EA Bruford 2004 The ABCs of solute carriers: physiological, pathological and therapeutic implications of human membrane transport proteins. *Pflugers Arch* **447** 465-468.

Jan, SZ, G Hamer, S Repping, DG de Rooij, AM van Pelt, and TL Vormer 2012 Molecular control of rodent spermatogenesis. *Biochim Biophys Acta* **1822** 1838-1850.

Kang-Decker, N, GT Mantchev, SC Juneja, MA McNiven, and JM van Deursen 2001 Lack of acrosome formation in Hrb-deficient mice. *Science* **294** 1531-1533.

Kierszenbaum, AL, and LL Tres 2004 The acrosome-acroplaxome-manchette complex and the shaping of the spermatid head. *Arch Histol Cytol* **67** 271-284.

Koscinski, I, E Elinati, C Fossard, C Redin, J Muller, J Velez de la Calle, F Schmitt, M Ben Khelifa, PF Ray, Z Kilani, CL Barratt, and S Viville 2011 DPY19L2 deletion as a major cause of globozoospermia. *Am J Hum Genet* **88** 344-350.

Liu, G, QW Shi, and GX Lu 2010 A newly discovered mutation in PICK1 in a human with globozoospermia. *Asian J Androl* **12** 556-560.

Matsuo, N, S Kawamoto, K Matsubara, and K Okubo 1997 Cloning of a cDNA encoding a novel sugar transporter expressed in the neonatal mouse hippocampus. *Biochem Biophys Res Commun* **238** 126-129.

Moreno, RD, and CP Alvarado 2006 The mammalian acrosome as a secretory lysosome: new and old evidence. *Mol Reprod Dev* **73** 1430-1434.

Natsume, W, K Tanabe, S Kon, N Yoshida, T Watanabe, T Torii, and M Satake 2006 SMAP2, a novel ARF GTPase-activating protein, interacts with clathrin and clathrin assembly protein and functions on the AP-1-positive early endosome/trans-Golgi network. *Mol Biol Cell* **17** 2592-2603.

Paiardi, C, ME Pasini, M Gioria, and G Berruti 2011 Failure of acrosome formation and globozoospermia in the wobbler mouse, a Vps54 spontaneous recessive mutant. *Spermatogenesis* **1** 52-62.

Pierre, V, G Martinez, C Coutton, J Delaroche, S Yassine, C Novella, K Pernet-Gallay, S Hennebicq, PF Ray, and C Arnoult 2012 Absence of Dpy19l2, a new inner nuclear membrane protein, causes globozoospermia in mice by preventing the anchoring of the acrosome to the nucleus. *Development* **139** 2955-2965.

Ratcliff, R, MJ Evans, J Doran, BJ Wainwright, R Williamson, and WH Colledge 1992 Disruption of the cystic fibrosis transmembrane conductance regulator gene in embryonic stem cells by gene targetting. *Transgenic Res* **1** 177-181.

Russell, LD, RA Ettlin, AP Sinha Hikim, and ED Clegg 1990 Histological and Histopathological Evaluation of the Testis. edn 1st Edition: Cache River Press.

Sreedharan, S, O Stephansson, HB Schioth, and R Fredriksson 2011 Long evolutionary conservation and considerable tissue specificity of several atypical solute carrier transporters. *Gene* **478** 11-18.

Toshimori, K, and C Ito 2003 Formation and organization of the mammalian sperm head. *Arch Histol Cytol* **66** 383-396.

Wang, H, H Wan, X Li, W Liu, Q Chen, Y Wang, L Yang, H Tang, X Zhang, E Duan, X Zhao, F Gao, and W Li 2014 Atg7 is required for acrosome biogenesis during spermatogenesis in mice. *Cell Res* **24** 852-869.

Xiao, N, C Kam, C Shen, W Jin, J Wang, KM Lee, L Jiang, and J Xia 2009 PICK1 deficiency causes male infertility in mice by disrupting acrosome formation. *J Clin Invest* **119** 802-812.

Xu, X, PA Toselli, LD Russell, and DC Seldin 1999 Globozoospermia in mice lacking the casein kinase II alpha' catalytic subunit. *Nat Genet* **23** 118-121.

Yao, R, C Ito, Y Natsume, Y Sugitani, H Yamanaka, S Kuretake, K Yanagida, A Sato, K Toshimori, and T Noda 2002 Lack of acrosome formation in mice lacking a Golgi protein, GOPC. *Proc Natl Acad Sci U S A* **99** 11211-11216.

Yassine, S, J Escoffier, G Martinez, C Coutton, T Karaouzene, R Zouari, JL Ravanat, C Metzler-Guillemain, HC Lee, R Fissore, S Hennebicq, PF Ray, and C Arnoult 2015 Dpy19l2-deficient globozoospermic sperm display altered genome packaging and DNA damage that compromises the initiation of embryo development. *Mol Hum Reprod* **21** 169-185.

Yildiz, Y, H Matern, B Thompson, JC Allegood, RL Warren, DM Ramirez, RE Hammer, FK Hamra, S Matern, and DW Russell 2006 Mutation of beta-glucosidase 2 causes glycolipid storage disease and impaired male fertility. *J Clin Invest* **116** 2985-2994.

Yoshida, T, SO Ioshii, K Imanaka-Yoshida, and K Izutsu 1994 Association of cytoplasmic dynein with manchette microtubules and spermatid nuclear envelope during spermiogenesis in rats. *J Cell Sci* **107 (Pt 3)** 625-633.

Figure Legends

Figure 1. Molecular characterization of *Mfsd14a* mutant mice.

A. Targetted *Mfsd14a* allele. The *Mfsd14a* gene consists of 12 exons (coding regions shaded). A 70bp deletion was introduced into exon 4 and an internal ribosome entry sequence (IRES)-*LacZ* transgene inserted to detect *Mfsd14a* gene expression by staining for β-galactosidase activity. Primer locations are indicated by arrows.

B. Confirmation of a null allele by RT-PCR of RNA from testes. PCR between exons upstream of the insertion (P1F/P3R) amplified products in wild-type and homozygous mutant samples. PCR amplification across exon 4 (P3F/P5R) gave a PCR product in the mutant that was generated from transcripts spliced between exons 3 and 5. PCR amplification downstream of the insertion (P4F/P5R) did not give a product in the mutant samples. *Hprt* was included as a positive control for the PCR reaction. –RT, no reverse transcriptase; –ve, no template control. M, Bioline 1Kb DNA marker.

C. *Mfsd14a* gene expression in the hippocampus visualized by β-galactosidase staining (blue). Scale bar = 0.25 cm.

D. *Mfsd14a* gene expression in the testes of mutant (-/-) mice visualized by β-galactosidase staining (blue). Staining was found in the cytoplasm of Sertoli cells (arrowheads indicate Sertoli cell nuclei). Scale bar = 50 μm.

Figure 2. Reproductive phenotype of mutant *Mfsd14a* male mice.

A. Plasma testosterone levels. Plasma testosterone concentrations were measured from terminal blood samples by ELISA. No significant difference was found between mutant (n=8) and wild-type males (n=8) ($P = 0.38$, Mann-Whitney test).

B. Copulatory plugging rate. *Mfsd14a* mutant mice (n=8) and control wild-type (n=8) males were housed singly with a wild-type female each and checked daily for a copulatory plug in the vagina.

C. Sperm counts. Sperm were isolated from the vas deferens of mutant (n=8) and wild-type (n=8) mice and counted. Mutant mice had a significantly lower number of sperm ($P<0.0001$, unpaired t-test with Welch correction).

D. Germ cell numbers. The number of cells in each germ cell category within seminiferous tubule sections at stages IV/V/VI of the seminiferous cycle was counted. Sg, spermatogonia; Sc, primary spermatocytes; Str, round spermatids; Ste, elongating spermatids. (n=4 for wild-type and mutant mice). The only significant difference was between the numbers of elongating spermatids ($P<0.001$, Mann-Whitney test).

Figure 3. Defective spermiogenesis and globozoospermia in *Mfsd14a* mutant mice.

A. Spermatogenesis in wild-type testis showing normal condensation of sperm heads (arrowed) after spermiogenesis. Scale bar = 50 μm.

B. Defective spermiogenesis in mutant testis with spermatozoa showing rounded heads (arrowed). Scale bar = 50 μm.

C. Resin section of epididymis from wild-type mice showing large numbers of normal sperm with hook shaped heads (arrowed). Scale bar = 50 μm.

D. Resin section of epididymis from mutant mice showing severely reduced sperm numbers with round heads (arrowed) and failure to remove excess cytoplasm. Scale bar = 50 μm.

E and F. Resin sections of stage I seminiferous tubules showing similar appearance of Step 1 spermatids and round-headed spermatozoa in mutants (F). Toluidine blue stain. Scale bars = 25 μm.

G and H. Resin sections of stage VI seminiferous tubules showing acrosome cap formation in wild-type (deep blue stain, arrowed, high power insert) but no acrosome formation in the mutants with with occasional vesicle accumulation (arrowed). Toluidine blue stain. Scale bar = 25 μm.

I. Normal morphology of sperm from wild-type mouse epididymis. Scale bar = 20 μm.

J. Round head morphology of sperm isolated from mutant mouse epididymis. Scale bar = 20 μm.

K and M. Location of mitochondria in mid-piece of sperm from wild-type mice visualised by MitoTracker Green stain. I, phase contrast; K, fluorescence. Scale bar = 40 μm.

L and N. Failure of mitochondria to correctly localise to mid-piece region of sperm in mutant mice visualised by MitoTracker Green stain. The mitochondria often remain in the residual cytoplasm that is not correctly removed from the sperm head. J, phase contrast; L, fluorescence. Scale bar = 40 μm.

Sg, spermatogonium; Sc, spermatocyte; Str, round spermatid; Ste, elongating spermatid, Sz, spermatozoon.

Figure 4. Ultrastructural analysis of spermiogenesis in *Mfsd14a* mutant mice.

Transmission electron microscopy illustrating different stages of spermiogenesis in wild-type (+/+) and mutant (-/-) mice. Micrographs were staged according to Russell *et al* (1990) (Russell, et al. 1990). All scale bars = 5 μM.

A. Step 1 spermatids showing no obvious difference between mutant and wild-type. nu = nucleus.

B. Step 6 spermatid showing juxtanuclear Golgi apparatus (G) and formation of the acrosomal cap (white arrow) with a single pro-acrosomal granule (asterisk) over the nucleus (nu) in the wild-type. Several vesicles containing pro-acrosomal granules (asterisk) can be seen in the mutant but with no fusion to form the acrosome. Mitochondria are indicated by black arrowheads.

C. Late stage Step 9 spermatid in which the nucleus (nu) has become ovoid and the acrosomal cap expands to cover the nucleus (white arrow) in the wild-type. Mutants have an abnormal nuclear shape and lack acrosome formation (white arrow). The manchette (m) has formed in both the wild-type and the mutants.

D. Step 13 of spermiogenesis showing condensed nuclear heads (nu) and acrosome (white arrow) in wild-type mice and misshapen and fragmented nuclei in the mutant mice with no apparent acrosome. Mitochondria are indicated by black arrowheads.

E. Spermatozoa in the epididymis showing condensed nuclei (nu) and overlaying acrosome cap (black arrowhead) in wild-type mice. Mutant spermatozoa showing abnormal shaped nuclei and round heads (globozoospermia) with a failure to remove residual cytoplasm (cyt).

524 Figure 1

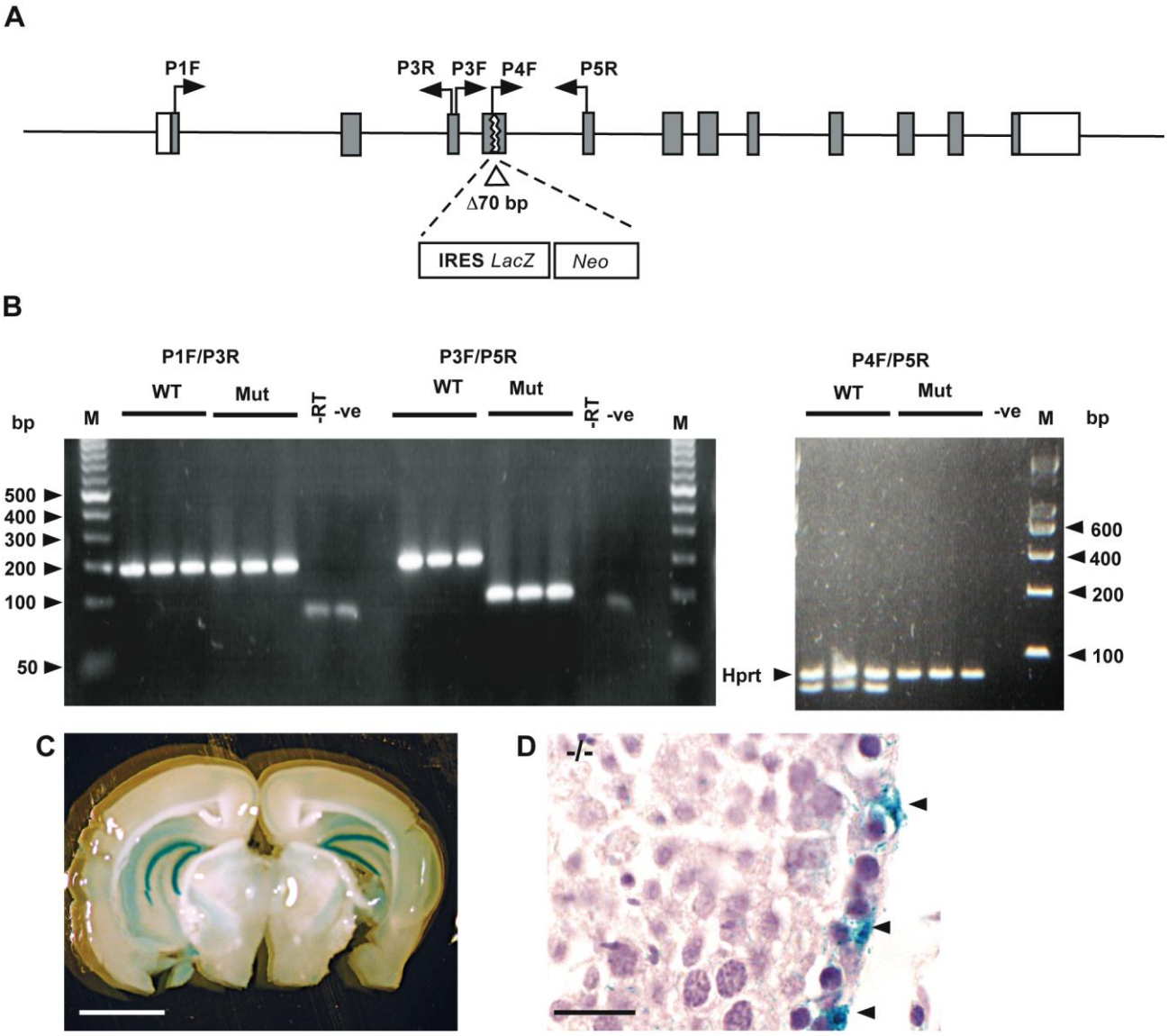

525

526

527 Figure 2

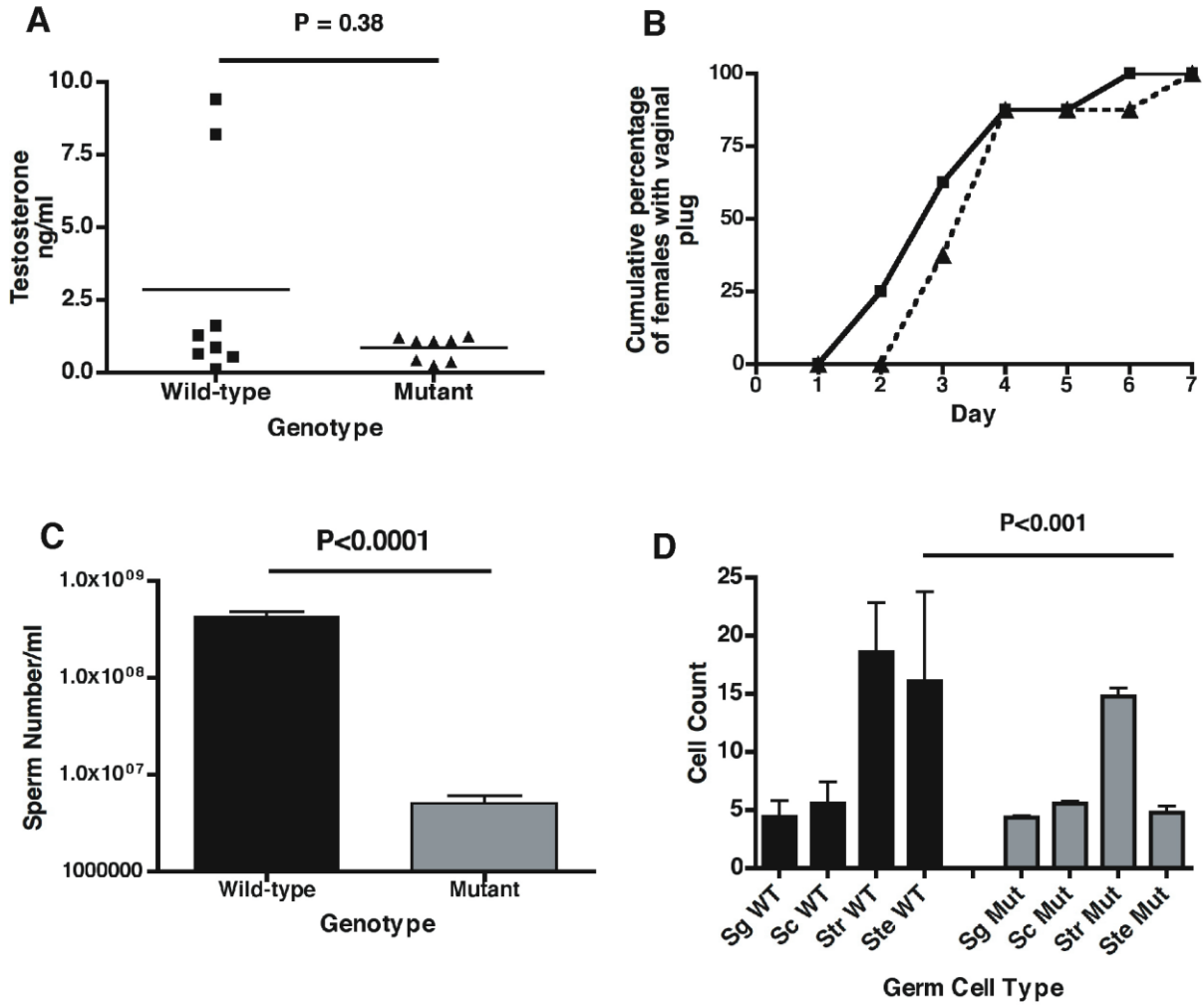

528

529

Figure 3

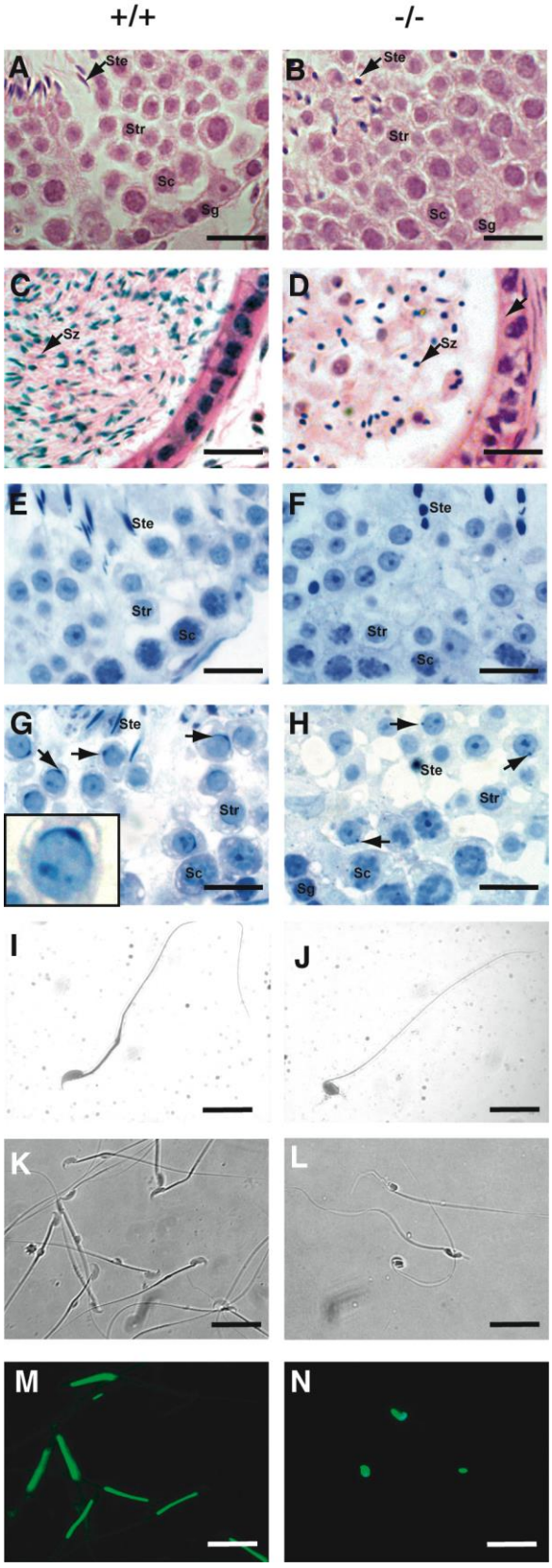
+/+
-/-
A
Ste
Str
Sc
Sg
B
Ste
Str
Sc
Sg
C
Sz
D
Sz
E
Ste
Str
Sc
F
Ste
Str
Sc
G
Ste
Str
Sc
H
Ste
Str
Sc
Sg
I
J
K
L
M
N

Figure 4

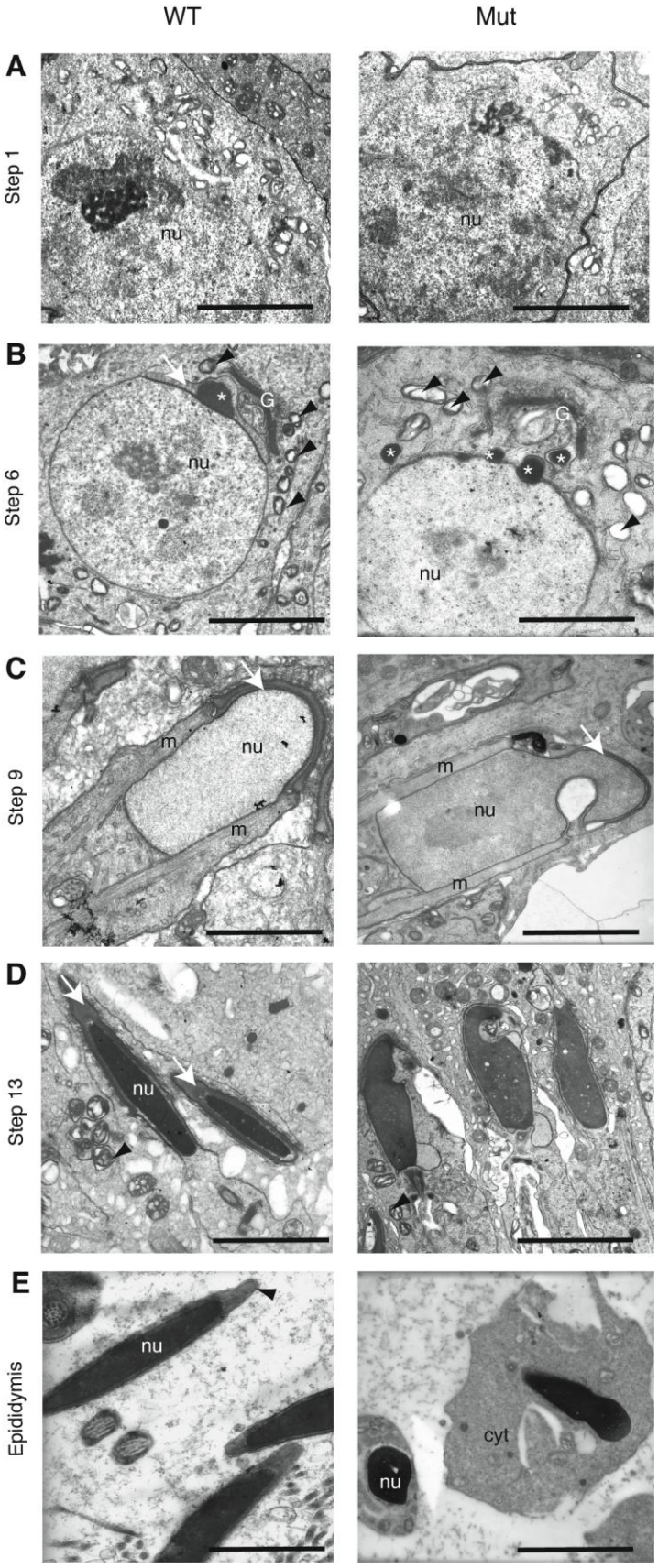
WT
Mut
A
Step 1
nu
nu
B
Step 6
G
nu
G
nu
C
Step 9
m
nu
m
m
nu
m
D
Step 13
nu
E
Epididymis
nu
cyt
nu